

Normal and oblique specular reflectivity of CuGeO_3

Néstor E. Massa

Laboratorio Nacional de Investigación y Servicios en Espectroscopía Óptica, Programa QUINOR-Departamento de Química and Departamento de Física, Universidad Nacional de La Plata, Casilla de Correo No. 962, 1900 La Plata, Argentina

Juan Campá

Departamento de Cristalografía y Mineralogía, Universidad Complutense de Madrid, 28040 Madrid, Spain

Isidoro Rasines

Instituto de Ciencia de Materiales-Consejo Superior de Investigaciones Científicas, Serrano 113, 28006 Madrid, Spain

(Received 25 October 1994; revised manuscript received 14 April 1995)

We report on the ac -plane specular reflectivity of CuGeO_3 as a function of the angle of incidence. While our spectra for near-normal incidence are those of an insulator, in the grazing-incident spectrum we found a broad continuum. This suggests that the b -direction response, that is, the response normal to the ac plane, is weakly metallic. We suggest the origin of this electronic anisotropy is due to impurity levels in the gap. We reason that its presence is due to oxygen vacancies in the chains and that this would justify, at least in part, some of the softening of the longitudinal acoustical mode recently reported by neutron-scattering measurements.

One-dimensional antiferromagnetic behavior of NiO_6 flat-tened chains, with short Ni-O-Ni distances and with the nearest oxygen to Ni bonds distorted from the 90° angle of a regular octahedron, is the main characteristic of $R_2\text{BaNiO}_5$, a family of compounds that is formally analogous to the green phases of $R_2\text{BaCuO}_5$.^{1,2} In these materials the structural features can be understood using a combination of results from molecular-orbital theory, tight-binding band-structure calculations, and empirical atom-atom potential arguments.³ Because of our interest in this kind of nearly one-dimensional magnetic interaction we decided to turn our attention to copper germanium trioxide (CuGeO_3). Its crystal structure is reported to be orthorhombic with room-temperature unit cell of dimension $a=4.81 \text{ \AA}$, $b=8.47 \text{ \AA}$, and $c=2.94 \text{ \AA}$.⁴ It contains CuO_6 chains along the orthorhombic c direction with Cu ions located at the centers of edge-sharing elongated oxygen octahedra between which the tetrahedrally coordinated Ge ions also form chains.⁴

CuGeO_3 , already known for some of its thermodynamic⁵ and magnetic resonance⁶ properties, has attracted a considerable degree of attention after being proposed as an inorganic spin- $\frac{1}{2}$ Peierls compound.⁷ Recently, there have been studies on electron paramagnetic resonance,⁸ neutron diffraction,⁹ and the electronic band structure of CuGeO_3 .¹⁰ A proposed magnetically induced transition was found at 14 K with the development of a 2.1 meV energy gap in the spin excitations.¹¹

Lorenzo *et al.*¹² have found, by neutron scattering, that the energy of the longitudinal acoustic mode along b^* lies below the measured transverse acoustic (TA) branch propagating in the same direction. They were able to measure down to $\mathbf{q}=(0,0.15,0)$ in spite of the difficulties caused by the small size of the crystal. Constant-energy scans demonstrate that there is no acoustic mode lying above the TA branch.¹² They also observed, below the reported magnetic transition at $T_c=14 \text{ K}$, evidence for the development of a spontaneous strain Δb that made them speculate that Δb ,

and not the spin gap, is the order parameter of the phase transition.¹² The softening of longitudinal acoustic phonons in a direction (along the b axis) perpendicular to the chains is not expected in a spin-Peierls system where the lattice dimerization is along the chain direction (c axis).¹²

A twist-type lattice dimerization in the a - b plane, perpendicular to the antiferromagnetic c axis, has also been claimed as the driving mechanism for the spin-Peierls transition.¹³ Pouget *et al.*¹⁴ reported x-ray- and elastic-neutron-scattering measurements that, indeed show that CuGeO_3 undergoes a second-order structural transition at $T_{\text{SP}}=14 \text{ K}$ at which the magnetic susceptibility abruptly decreases. Sugai¹⁵ reported broad two-magnon Raman scattering, suggesting that spin correlations are two dimensional.

Here we discuss specular far-infrared reflectivity measurements at 300 K taken at several angles of incidence that reveal some anomalies in phonon frequencies. These can be understood as due to distorted tetrahedra and octahedra in the chains. We also report on unusual strength in some of the zone-center longitudinal optical (LO) phonons and an electronic anisotropy along the crystallographic b direction perpendicular to the orthorhombic ac plane.

The growth habit of CuGeO_3 is such that the crystals are elongated along the c axis and thin along the b axis. Thus the samples are thin plates with well-defined ac -plane faces making difficult normal reflectivity measurements polarized in the b crystallographic direction. For this reason we opted to use oblique incident radiation to infer the far-infrared spectrum in the b direction.¹⁶ This kind of measurement also reveals longitudinal excitations present in a system.

Single crystals of CuGeO_3 were grown from stoichiometric mixtures of reagent-grade CuO and GeO_2 which were heated up to 1040°C , maintained as a melt at this temperature for 4 h and cooled to 940°C at 4°C/h . The resulting turquoise thin plates were mounted in an ENRAF-NONIUS CAD4 single-crystal diffractometer. Refining by least-squares fitting, with the 2θ values of 25 reflections obtained

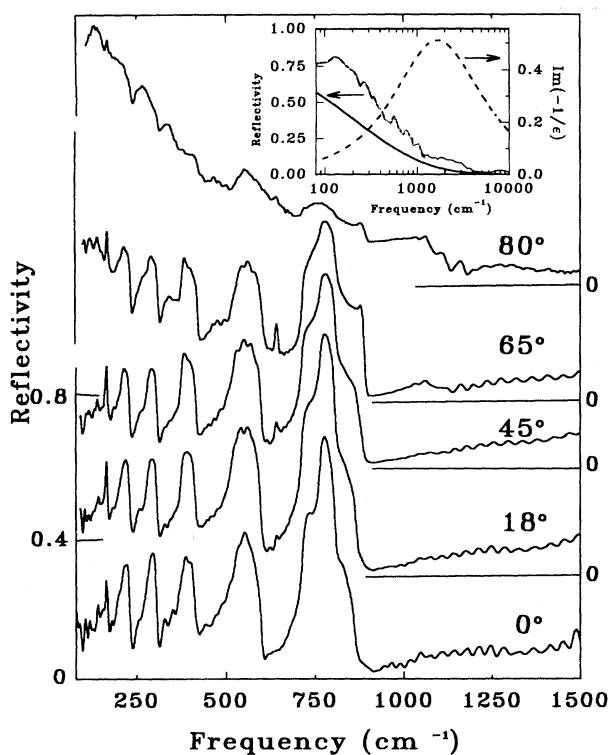


FIG. 1. Room-temperature ac -plane reflectance of CuGeO_3 as a function of frequency for various angles of incidence. The inset semilogarithmic graph shows (full line) the fit using a Drude model with two damping constants. The dashed line is the calculated loss function.

using graphite-monochromated $\text{Mo } K\alpha_1$, $\lambda = 0.71069 \text{ \AA}$, yielded $a = 4.7940(9) \text{ \AA}$, $b = 8.460(1) \text{ \AA}$, and $c = 2.940(1) \text{ \AA}$ for the lattice parameters of this compound. These are in agreement with published results⁴ and are used to assign the D_{2h}^5 - $Pmmb$ orthorhombic space group to CuGeO_3 .

Our reflectivity measurements were done in a FTIR Bruker 133v interferometer with an as-grown composite made of three nearly parallel CuGeO_3 rods. This arrangement provided a platelike specimen of $3 \times 7 \text{ mm}^2$ little more than 1 mm thick. The sample was mounted on a device that allows continuous change of the angle of incidence of the radiation from 10° to 80° .

Near-normal reflectivity from ambient temperature to 80 K was measured with the sample glued to the cold finger of an Oxford DN 1754 cryostat. Transmission measurements have been done with pellets made of spectroscopic-grade CsI or polyethylene with microcrystallites of CuGeO_3 diluted in them. All measurements were done in vacuum.

We used a fresh surface aluminum mirror as 100% reference. The use of deuterated triglycine sulfate (DTGS) detectors in the whole frequency range in conjunction with the small size of our samples preclude us from doing polarized measurements in other than the frequency range higher than 600 cm^{-1} where we were able to also use a liquid-nitrogen-cooled HgCdTe detector.

Figure 1 shows our spectra at several angles of incidence.

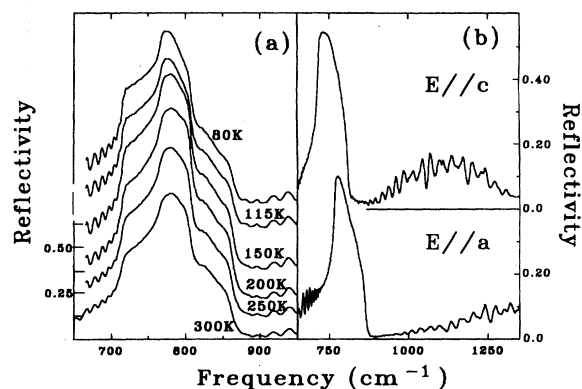


FIG. 2. (a) Temperature dependence of the ac -plane depolarized spectrum in the stretching-mode frequency region. (b) Polarized spectra at 80 K.

The room-temperature spectrum at near-normal incidence shows the band profile of an insulator.

The measured bands for normal reflectivity, and their frequency positions, are similar to those reported for BaBiO_3 ,¹⁷ and the interpretation is similar. The number of the strongest features agrees with the expected phonons in the ac plane, four $B_{1u}(c)$ and five $B_{3u}(a)$, for a crystal with two molecules per unit cell in the space group $Pmmb$. The band centered at about 780 cm^{-1} , shown in detail in Fig. 2(a), is assigned to the stretching vibrational mode corresponding to the triply degenerate F_{1u} mode of the prototype cubic perovskite. We verified the excellent reproducibility of that band profile with an infrared microscope attached to a Bruker 66 interferometer comparing the signal of our sample with the reflectivity from $130 \mu\text{m}$ spots of smaller, macroscopically perfect CuGeO_3 single crystals.

We also note that the higher-frequency side of the spectrum for near-normal incidence (to the ac plane) shows a wavy modulation and that it changes with the angle of incidence. Since, on the other hand, our crystals easily cleave in very thin morphologically perfect ac plates we interpret that effect as an interference pattern produced by the reflection of radiation by planes of CuGeO_3 . The sinusoidal pattern shows the behavior of a stratified medium giving the imprint of a layered compound.

In a finding that seems to be in disagreement with what is suggested in Ref. 13, lower-temperature measurements down to 80 K, shown in Fig. 2(a) for the band centered at 780 cm^{-1} , do not reveal features other than the decrease of damping expected for a molecular polar crystal. Polarized measurements resolving this feature in two bands are shown in Fig. 2(b) at 80 K for $\mathbf{E} \parallel c$ and for $\mathbf{E} \parallel a$. The asymmetric profiles are due to a systematic misalignment of the rods inducing a shoulder due to the third b -active stretching B_{2u} mode, shown in Fig. 3 at 870 cm^{-1} in transmission of crystallites at 80 K. Here we see that the two first vibrational groups have the B_{2u} b -active modes at much higher frequencies than the other two, indicating octahedra having a $\text{Cu-O}(1)$ bond, where $\text{O}(1)$ is the apex oxygen, longer than the planar ones in the ac plane, as reported from x-ray-diffraction measurements.⁴ In addition, our 80 K transmission and depolarized normal reflectivity measurements (due

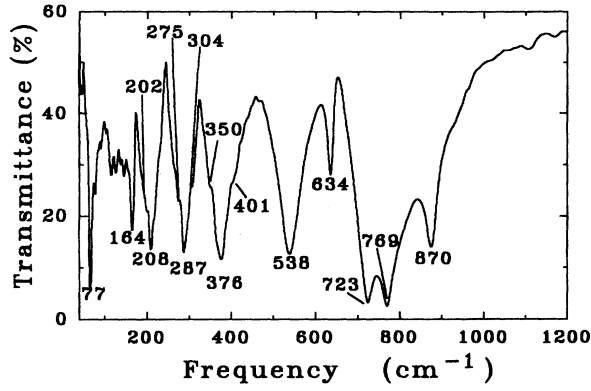


FIG. 3. Depolarized background-corrected transmission measurement of CuGeO_3 crystallites at 80 K.

to the small size of our samples we were unable to measure the polarized low frequency) have band profiles resolving a weaker shoulder that suggests a lower symmetry for CuGeO_3 than the space group $Pmmb-D_{2h}^5$.

The measurements for $\mathbf{E} \parallel c$, Fig. 2(b), also show an extra band centered at 1150 cm^{-1} . This, and recent reflectivity measurements¹⁸ that report phonon anomalies in oxides due to phonon coupling to spin excitations, led us to believe that it is reasonable to speculate that this feature is related, due to its frequency position and half width at half maximum, to a spin interaction of some sort.

A quantitative analysis of the dielectric function and phonon frequency positions, shown in Fig. 4 and Table I, has been done by fitting the measured data. Knowing the normal-incidence reflectivity and representing phonons by Lorentzian oscillators in the classical formulation for the complex dielectric function $\epsilon(\omega)_{ac}$,¹⁹

$$\epsilon_{ac}(\omega) = \epsilon_{\infty} \prod_{j=1}^N \frac{\Omega_{jLO}^2 - \omega^2 - i\gamma_{jLO}\omega}{\Omega_{jTO}^2 - \omega^2 - i\gamma_{jTO}\omega}, \quad (1)$$

we calculate the high-frequency dielectric constant ϵ_{∞} ; Ω_{jTO} and Ω_{jLO} are the transverse and longitudinal j th optical phonon frequencies, and γ_{jTO} and γ_{jLO} their transverse and longitudinal damping constants. Table I also has the oscillator strengths S_j calculated from

$$S_j = \Omega_{jTO}^{-2} \frac{\left(\prod_k \Omega_{kLO}^2 - \Omega_{jTO}^2 \right)}{\left(\prod_{k \neq j} \Omega_{kTO}^2 - \Omega_{jTO}^2 \right)}. \quad (2)$$

Figure 1 also shows reflectivity spectra of CuGeO_3 as the angle of incidence of the radiation is increased. For 45° , and clearly for the angle of incidence at 65° , distinctive sharp small bands appear at 634 and 870 cm^{-1} . These correspond to the frequencies of the B_{2u} transverse optical modes already shown in transmission in Fig. 3. We also note that, while the band at 634 cm^{-1} , being very sharp, seems to lack the macroscopic field associated with its longitudinal mode, the one at 870 cm^{-1} , which appears as an underdamped polar phonon, once again characteristic of an insulator, has a

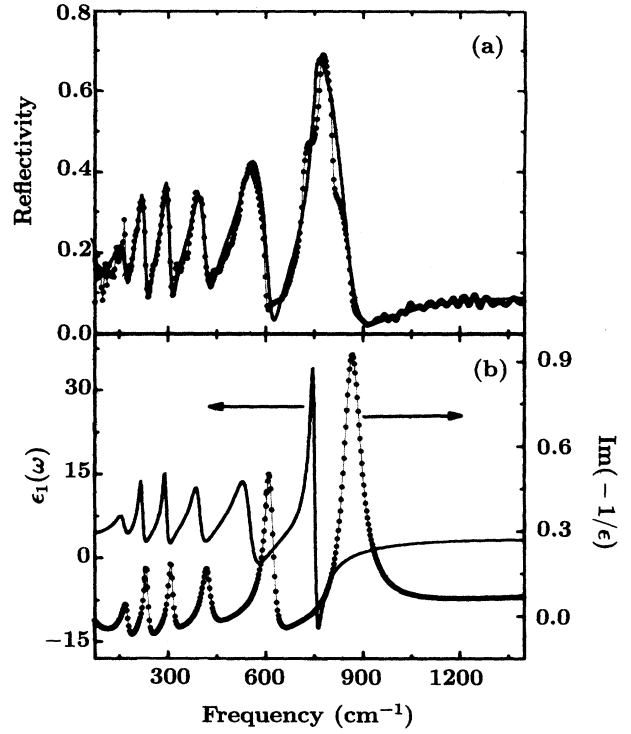


FIG. 4. (a) Near-normal-incidence reflectivity spectrum of CuGeO_3 . Dotted line, data; full line, fitted. (b) Full line, real part of the dielectric function; dotted line, loss function.

very sharp edge at 900 cm^{-1} . Figure 5 shows in detail this edge enhancement as a function of angle of incidence. We understand that enhancement as due to the Berreman effect,²⁰ where zone-center longitudinal optical modes can be seen with radiation incident obliquely. Dean Sciacca *et al.*²¹ have recently briefly reviewed this point. Their reasoning may be extended to reflectivity measurements of more complex mo-

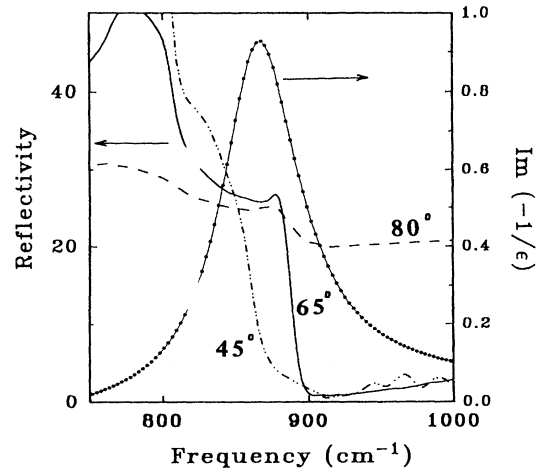


FIG. 5. Sharp-cutoff enhancement of the 900 cm^{-1} longitudinal optical mode of CuGeO_3 at room temperature as a function of the angle of incidence. The dotted line is the calculated loss function.

TABLE I. Multioscillator fit dispersion parameters. $\epsilon_\infty=2.23$. An agreement within 5% is achieved between the frequencies of the transverse optical [$\Omega_{\text{TO}}(^*)$] modes calculated from the multioscillator fit and those measured in the transmission spectrum [$\Omega_{\text{TO}}(^*)$]. This error band may also be extended to the longitudinal optical modes and the damping fitting parameters. The numbers in parentheses are the frequencies from the fit to the polarized spectra shown in Fig. 2.

$\Omega_{\text{TO}}(^*)$ (cm ⁻¹)	$\Omega_{\text{TO}}(^{**})$ (cm ⁻¹)	γ_{TO} (cm ⁻¹)	Ω_{LO} (cm ⁻¹)	γ_{LO} (cm ⁻²)	S_j (cm ⁻¹)
75.9	77	182.9	79.4	126.9	0.53
165.5	164	27.8	173.9	20.9	0.63
220.7	208	14.7	235.2	15.8	0.62
294.3	288	14.4	310.0	17.2	0.42
396.4	376	30.1	422.8	29.61	0.48
552.7	538	32.5	615.6	32.5	0.53
750.9 (720.0)	723	16.3 (20.4)	778.0 (789.0)	2794.9 (25.8)	0.23 (0.36)
805.2 (779.0)	769	1317.6 (27.3)	865.5 (852.0)	58.9 (48.4)	0.13 (0.55)

lecular crystals having polar vibrations. A quantitative analysis for a uniaxially anisotropic medium can be found in Ref. 22.

A broad background emerges in the spectrum for angle of incidence of 45°. The screening of the phonon structure starts at this angle as is shown in Fig. 1. For radiation directed at a near-grazing angle of about 80°, the spectrum exhibits the band profile expected of free carriers. It has an “edge” at 1150 cm⁻¹ near the broad weaker band found for (E||c) in Fig. 2(b).

Since our results from the *ac* plane show the spectra of an insulator, the electronic anomaly has to originate from the direction perpendicular to it, i.e., parallel to the *b* axis, in the *ab* plane of CuGeO₃. This feature which we believe is strongly enhanced by the large angle of incidence, suggests that CuGeO₃, when doped with suitable impurities, will undergo a transition into a conducting oxide system. It is then tempting to calculate what would be the carrier contribution assuming a fit of the spectrum taken at 80° to a continuum Drude-like model in the *b* direction and a regular multioscillator expansion, as in Eq. (1), for the *s* reflectivity perpendicular to the plane of incidence. Thus for the extraordinary *p* reflectivity we take the contribution of a plasma to the dielectric function²³ with two damping constants given by

$$\epsilon_{1e} + i\epsilon_{2e} = \epsilon_\infty \frac{(\Omega_{\text{pl}}^2 - \omega^2 + i\gamma_{\text{pl}}\omega)}{(-\omega^2 + i\gamma_0\omega)}, \quad (3)$$

with Ω_{pl} for the plasma frequency, γ_p its damping, and γ_0 understood as a phenomenological damping introduced by the lattice drag. When these two dampings are set to equal each other, one retrieves the classical Drude formula.

Since the real refractive index is calculated from ϵ_{1e} and ϵ_{2e} , the reflection coefficients r_e and r_{ac} may then be computed from²²

$$r_e = \frac{n_{ac}n_e \cos\varphi_i - \sqrt{n_e^2 - \sin^2\varphi_i}}{n_{ac}n_e \cos\varphi_i + \sqrt{n_e^2 - \sin^2\varphi_i}}, \quad (4)$$

and

$$r_{ac} = \frac{\cos\varphi_i - \sqrt{n_{ac}^2 - \sin^2\varphi_i}}{\cos\varphi_i + \sqrt{n_{ac}^2 - \sin^2\varphi_i}} \quad (5)$$

where n_c and n_{ac} are the *p* complex refractive index and the *s* complex refractive index, respectively. φ_i is the angle of incidence. A depolarized effective reflectivity can then be written as

$$R = \frac{1}{2} \sqrt{|r_e|^2 + |r_{ac}|^2}, \quad (6)$$

where the factor 1/2 takes into account the depolarized nature of our measurements.

The reflectivity fit of the spectrum for $\varphi_i=80^\circ$ (Fig. 1), using Eq. (6), yields $\Omega_{\text{pl}}=174$ cm⁻¹, $\gamma_p=45.17$ cm⁻¹, and $\gamma_0=421.21$ cm⁻¹. The value of the high-frequency dielectric constant now is $\epsilon_\infty=1.01$. The plasma contribution extracted from this fit and the calculated loss function are shown in a semilogarithmic scale in the inset of Fig. 1.

With

$$\Omega_{\text{pl}}^2 = 4\pi e^2 N/m^*, \quad (7)$$

we can estimate an effective carrier concentration $N^*=Nm/m^*$ (m and m^* are the free- and effective electron mass; N and N^* the number and the effective number of carriers, respectively). Taken as an upper limit, this yields $N^*=3.44 \times 10^{17}$, about four orders of magnitude less than $N^*=5.4 \times 10^{21}$ found by Travaglini *et al.*²⁴ for the quasi-one-dimensional metal K_{0.3}MoO₃. If we recall that low-dimensional metal oxides in many cases present morphological crystal anisotropies with a high conductivity channel, we may infer that our measurements suggest that defect-induced carriers ought to be considered in explaining the softening found in neutron-scattering measurements in the longitudinal mode along the *b* axis.

Oxygen vacancies may generate impurity levels in the gap allowing a low concentration of free carriers without shielding the phonon structure found in a far-infrared normal-incident measurement. Mattheiss also suggested a potential specialized channel of conduction for GeCuO₃ that in the perfect material would be inhibited because of the need to tunnel through nodal charge-density regions along the chains.¹⁰

We also conclude that oxygen defects are present in the chains of CuGeO₃ because of our results on the infrared and transport properties of the layered perovskite-related oxide Ba₅Nb₄O₁₅, and its oxygen-deficient phases.²⁵ Here, their presence, introduced in this case by reduction in a controlled

atmosphere, shows strong luminescence that is excited with the infrared Nd YAG laser line (1.16 eV), where YAG is yttrium aluminum garnet, or the visible Ar⁺ laser lines (~1.48 eV). This peaks at 2000 cm⁻¹ when using the 5145 Å line. As reported by Sugai¹⁵ for this wavelength, our sample of CuGeO₃ also has a Raman background increase when the temperature is lowered. It is a broad band that extends beyond that frequency, indicating that in any interpretation beyond one involving only one intrachain magnetic interaction, although difficult to quantify and not mentioned in the recent literature, defects should also be considered before a conclusion on the true mechanism for the 14 K phase transition can be reached. The introduction of defects also explains the reported contradictory results for resistivities measured in single crystals and reduced ceramic samples.^{6,26} On the other hand, our findings suggest that properly reduced or doped CuGeO₃ may be a compound with interesting properties.

Summarizing, we report on the *ac*-plane specular reflectivity of CuGeO₃ as a function of the angle of incidence.

While our spectra for near-normal incidence are those of an insulator, in the grazing-incident spectrum we found a broad continuum. This suggests that the *b*-direction response, that is, the response normal to the *ac* plane, is weakly metallic. We suggest that the origin of this electronic anisotropy is due to impurity levels in the gap. We reason that their presence is due to oxygen defects in the chains and that this would explain, at least in part, some of the softening in the longitudinal acoustic mode recently reported by neutron-scattering measurements. Larger CuGeO₃ samples grown in a strongly controlled environment are needed to perform a more quantitative analysis of the spectral feature discussed in the present manuscript.

This research has been partially supported by Grant No. PID 3956/92 and a grant of the National Research Council of Argentina (CONICET) to Programa QUINOR. Financial support of the Spanish CICYT (Comisión Interministerial de Ciencia y Tecnología) under Project No. MAT92-0168 is also acknowledged.

-
- ¹J. Amador, E. Gutiérrez Puebla, M. A. Monge, I. Rasines, J. A. Campá, J. M. Gómez de Salazar, and C. Ruiz Valero, *Solid State Ionics* **32–33**, 123 (1989).
- ²J. Amador, E. Gutierrez Puebla, M. A. Monge, I. Rasines, and C. Ruiz Valero, *Phys. Rev. B* **42**, 7918 (1990).
- ³J. K. Burdett and J. F. Mitchell, *J. Am. Chem. Soc.* **112**, 6571 (1990).
- ⁴H. Völlenkle, A. Wittmann, and H. Nowotny, *Monatsh. Chem.* **98**, 1352 (1967).
- ⁵W. Weppner, C. Li-Chuan, and A. Rabenau, *J. Solid State Chem.* **31**, 257 (1980).
- ⁶G. A. Petrakovskii *et al.*, *Zh. Éksp. Teor. Fiz.* **98**, 1382 (1990) [*Sov. Phys. JETP* **71**, 772 (1990)].
- ⁷M. Hase, I. Terasaki, and K. Uchinokura, *Phys. Rev. Lett.* **70**, 3651 (1993).
- ⁸S. Oseroff, S.-W. Cheong, A. Fondado, B. Atkas, and Z. Fisk, *J. Appl. Phys.* **75**, 6819 (1994).
- ⁹M. Nishi, *J. Phys. C* **6**, L19 (1994).
- ¹⁰L. F. Mattheiss, *Phys. Rev. B* **49**, 14 050 (1994).
- ¹¹M. Hase, I. Terasaki, and K. Uchinokura, *Phys. Rev. Lett.* **70**, 3651 (1993).
- ¹²J. E. Lorenzo, K. Hirota, G. Shirane, J. M. Tranquada, M. Hase, K. Uchinokura, H. Kojima, I. Tanaka, and Y. Shibuya, *Phys. Rev. B* **50**, 1278 (1994).
- ¹³M. Arai, M. Fujita, K. Ubukata, H. Ohta, M. Motokawa, T. Otomo, K. Ohya, M. Mino, J. Akimitsu, and O. Fujita (unpublished).
- ¹⁴J. P. Pouget, L. P. Regnault, M. Ain, B. Hennion, J. P. Renard, P. Veillet, G. Dhalenne, and H. Revcolevschi, *Phys. Rev. Lett.* **72**, 4037 (1994).
- ¹⁵S. Sugai, *J. Phys. Soc. Jpn.* **62**, 3829 (1993).
- ¹⁶J. H. Kim, B. J. Feenstra, H. S. Somal, D. van der Marel, W. Y. Lee, A. M. Gerrits and A. Wittlin, *Phys. Rev. B* **49**, 13 065 (1994).
- ¹⁷J. Yh W. de Hair and G. Blasse, *Solid State Commun.* **12**, 727 (1973). Also, S. Uchida, S. Tajima, A. Masaki, S. Sugai, K. Kitazawa, and S. Tanaka, *J. Phys. Soc. Jpn.* **54**, 4395 (1985).
- ¹⁸Recent examples of spin-related features measured by infrared spectroscopy were reported by A. P. Litvinchuk, C. Thomsen, and M. Cardona, *Solid State Commun.* **83**, 343 (1992); C. C. Homes, M. Ziaei, B. P. Clayman, J. G. Irwin, and J. P. Franck, *Phys. Rev. B* **51**, 3140 (1995); *Bull. Am. Phys. Soc.* **40**, 1 (1995).
- ¹⁹T. Kurosawa, *J. Phys. Soc. Jpn.* **16**, 1208 (1961).
- ²⁰D. W. Berreman, *Phys. Rev.* **130**, 2193 (1963).
- ²¹M. Dean Sciacca, A. J. Mayor, Eunsoon Oh, A. K. Ramdas, and S. Rodriguez, *Solid State Commun.* **88**, 711 (1993); M. Dean Sciacca, A. J. Mayor, Eunsoon Oh, A. K. Ramdas, S. Rodriguez, J. K. Furdyna, M. R. Melloch, C. P. Beetz, and W. S. Yoo, *Phys. Rev. B* **51**, 7744 (1995).
- ²²A. Röseler, *Infrared Spectroscopic Ellipsometry* (Akademie-Verlag, Berlin, 1990).
- ²³F. Gervais, J. L. Servoin, A. Baratoff, J. G. Bednorz, and G. Binnig, *Phys. Rev. B* **47**, 8187 (1993), and references therein.
- ²⁴G. Travaglini, P. Wachter, J. Marcus, and C. Schlenker, *Solid State Commun.* **37**, 599 (1981).
- ²⁵A preliminary report can be found in S. Pagola, N. E. Massa, G. Polla, G. Leyva, and R. E. Carbonio, *Physica C* **235–240**, 755 (1994).
- ²⁶T. Hashemi, J. Illingsworth, and A. W. Brinkman, *J. Mater. Sci. Lett.* **11**, 255 (1992).